Paper

Int'l J. of Aeronautical & Space Sci. 16(4), 602–613 (2015)
DOI: http://dx.doi.org/10.5139/IJASS.2015.16.4.602

IJASS
International Journal of Aeronautical and Space Sciences

Performance Evaluation of Hinge Driving Separation Nut-type Holding and Releasing Mechanism Triggered by Nichrome Burn Wire

Myeong-Jae LEE*

Space Technology Synthesis Laboratory, Department of Aerospace Engineering, Chosun University, Gwangju 61452, Republic of Korea

Yong-Keun LEE**

Optronics System Group, Hanwha Thales, Gyeonggi-do 13494, Republic of Korea

Hyun-Ung OH***

Space Technology Synthesis Laboratory, Department of Aerospace Engineering, Chosun University, Gwangju 61452, Republic of Korea

Abstract

As one of the mission payloads to be verified through the cube satellite mission of Cube Laboratory for Space Technology Experimental Project (STEP Cube Lab), we developed a hinge driving separation nut-type holding and releasing mechanism. The mechanism offers advantages, such as a large holding capacity and negligible induced shock, although its activation principle is based on a nylon cable cutting mechanism triggered by a nichrome burn wire generally used for cube satellite applications for the purpose of holding and releasing onboard appendages owing to its simplicity and low cost. The basic characteristics of the mechanism have been measured through a release function test, static load test under qualification temperature limits, and shock measurement test. In addition, the structural safety and operational functionality of the mechanism module under launch and on-orbit environments have been successfully demonstrated through a vibration test and thermal vacuum test.

Key words: Non-explosive holding and release mechanism, Nichrome burn wire, Cube satellite

1. Introduction

The cube satellite program is an international, educational, and practical project proposed by Professor Robert Twiggs, of Stanford University. The cube satellite is a type of cube-shaped pico-class miniaturized satellite and is considerably smaller than typical commercial satellites. This type of satellite usually has a volume of 10 cm^3 for a standard size of one unit (1U), a mass of less than 1.33 kg, and typically uses commercial off-the-shelf components [1]. Recently, cube satellites have been used for increasingly complex missions [2-5], and their functionality, in an extremely small package gives rise to numerous mechanisms and deployable structures that are necessary for achieving challenging mission-related functions. The cube satellite architecture also requires that deployable structures such as solar arrays, antennas, and other appendages, are stowed for launch, released, and deployed in orbit for operation. The appendages require holding and release mechanisms that can provide adequate strength and stiffness to survive under the launch environment, as well as release functions to allow the deployment of these appendages in orbit.

Recently, various holding and release mechanisms have been developed for the separation of the appendages.

* Master's Course Student
** Chief Engineer
*** Professor, Corresponding author: ohu129@chosun.ac.kr

Received: September 9, 2015 Revised: December 18, 2015 Accepted: December 22, 2015

http://ijass.org pISSN: 2093-274x eISSN: 2093-2480

Pyrotechnic devices are widely used in the aerospace engineering field, especially for commercial satellite separation, holding, and release of appendages, owing to their high strength, stiffness, and successful deployments in space missions. However, these devices often induce a high-level of dynamic responses owing to the sudden transient release of strain energy. This high-frequency pyroshock sometimes causes malfunctions of electrical components or critical damage to the brittle components of a launch vehicle or satellite, resulting in mission failure [6]. The issue of the large shock generated by the pyrotechnic device becomes even more critical for pico-class satellites. The use of pyrotechnic devices as a separation mechanism for pico-satellites may easily cause problems because the external and internal parts are in closer physical proximity to the source of shock in pico-satellites than in larger satellites, owing to the extremely small size and volume of pico-satellites. Additionally, the cube satellite requirements do not allow the use of explosive pyro devices.

To reduce the shock caused by pyrotechnic devices, several types of non-explosive separation devices using a shape memory alloy (SMA) [7-9] have been developed and used in actual space missions [10, 11]. The advantages of the non-explosive actuators are their lower shock, higher load capability, and reusability for additional cycles after a simple reset. However, even though the shock level is small, the use of these devices may still have some limitations in cube satellites because of their high cost and the fact that they do not meet typical pico-satellite requirements of low weight, small size, and generating relatively small shocks. The high cost of these devices makes them impractical to use on cube satellites that have development cost limitations.

A nylon cable has been widely used as a mechanical constraint on the deployable appendages for cube satellite applications owing to its simplicity and low cost. This mechanical constraint is released by cutting the nylon cable using a nichrome burn wire. Nakaya et al. [12] developed a cable-cutting separation mechanism for cube satellite separation from the launcher. The four jaws of the mechanism that holds the cube satellite during launch are tightened by the nylon cable, which is then cut by heating a nichrome wire. Thurn et al. [13] developed a burn wire release mechanism to release two carpenter tape deployments and a stacer and tether deployment system. It utilizes a compression spring system to apply a force and a stroke to the nichrome burn wire for safer release. They conducted functional performance tests in vacuum conditions with the qualification temperature range of from -50°C to 70°C. The test results show a shorter cut time of the burn release mechanism under vacuum conditions than under air conditions. The turnstile antenna developed by Gomspace [14] consists of four monopole antennas with nearly omni-directional coverage. All four antenna elements are individually fixed by a nylon cable and released by the activation of burn resistors.

Generally, these devices meet many of the basic requirements for appendage separation on cube satellites. However, system complexity is unavoidable when it is applied to cube satellites with multiple deployable structures. In some cases, where more than one heated nichrome burn wire is used, synchronous release is an important factor for mission success. A smaller constraint force is also one of the disadvantages of the mechanism. These drawbacks mentioned above are compelling motives for the investigation and development of new approaches for a holding and release mechanism for cube satellite applications. To overcome the drawbacks mentioned above, Oh et al. [15] developed a segmented nut-type holding and release mechanism for cube satellite applications with the advantages of a high load capacity and negligible shock. The nut segment, which is built up by winding nylon cable around it, is released by cutting the nylon cable using the nichrome burn wire. The effectiveness of the design was verified through a functionality test and a static load test under qualification temperature limits on a demonstration model of the mechanism.

In this study, a new version of the separation nut-type holding and release mechanism is proposed and investigated, which is simpler than the one proposed by Oh et al. [15]. It does not require an outer housing with Velcro fasteners to avoid interference between the released nut and the constraint bolt immediately after separation. This mechanism will be one of the main payloads to be verified through the Cube Laboratory for Space Technology Experimental Project (STEP Cube Lab) mission [16]. This is the first pico-class satellite to be developed at the Space Technology Synthesis Laboratory (STSL) at Chosun University and is scheduled to be launched in 2015. To measure the basic characteristics of the newly proposed mechanism, we performed a function test, static test, and shock measurement test on the mechanism level. In this study, the mechanism module design, considering the on-orbit verification of the safety function of the mechanism through the STEP Cube Lab mission was proposed and investigated. The structural safety and normal operation of the mechanism under launch and on-orbit environments were verified through vibration test and thermal vacuum test under the qualification level. These qualification test results indicated that the proposed mechanism functions as intended in the design.

2. Hinge Driving Separation Nut-type Holding and Releasing Mechanism

2.1 Operating Principle of Mechanism

Figure 1 shows both the stowed and released configurations of the segmented nut-type holding and release mechanism developed in the previous study [15] for cube satellite applications, with the corresponding demonstration model is shown in Fig. 2. The mechanism was made out of Al-6061 and composed of a segmented nut, an M6 constraint bolt, a nylon cable, a nichrome burn wire, a separation spring, and a housing with Velcro fasteners. The segmented nut was mechanically constrained by winding the nylon cable around it, and the Velcro strips were attached to the surface of the integrated nut and the inside the housing, as shown in Fig. 2. To facilitate wrapping the nylon cable, V-shaped grooves are carved in the surface of the nut. The constraint bolt was screwed into the nut through the housing, which constrained the deployed appendages to which the housing is attached, as shown in Fig. 1(a). The nichrome burn wire was used as an actuator to release the mechanical constraint between the segmented nut and the constraint bolt. The segments of the nut, which were released by triggering the nichrome burn wire, moved radially outwards and were attached to the outer housing with Velcro strips by the restoration force of the separation springs compressed inside the nut, as shown in Fig. 1(b). The effectiveness of the mechanism design was verified under qualification temperature limits through a function test and a static load test of a demonstration model of the mechanism.

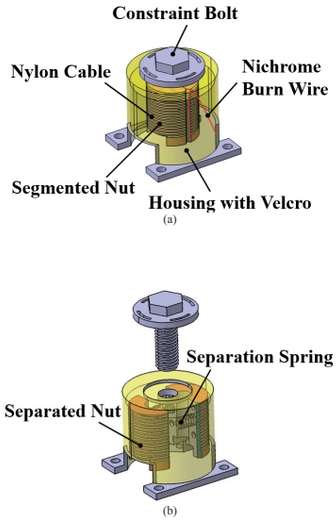

Fig. 1. Configuration of a segmented nut-type holding and release mechanism [15] ((a): Holding state, (b): Release state)

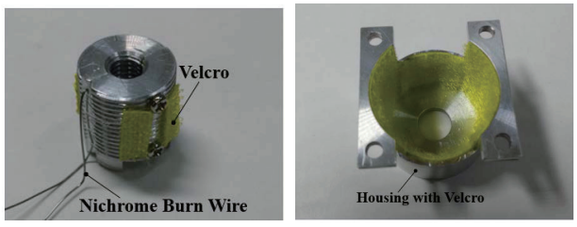

Fig. 2. Demonstration model of a segmented nut-type holding and release mechanism [15] ((a): Integrated nut, (b): Inside of housing)

Figure 3 shows the holding and released configurations of the new version of the hinge driving separation nut-type holding and releasing mechanism investigated in this study. The separation nut was constrained by winding the nylon cable around it, and the constraint was released by triggering the nichrome burn wire, similar to the conventional mechanism shown in Fig. 1. Separation springs were compressed inside the separation nut. When the nichrome burn wire was heated, the nylon cable wound around the integrated nut is cut and the nut is subsequently separated by the restoration force of the two separation springs. The separation springs allow the release of the constraint bolt when the segments of the separated nut rotate away from the bolt around the hinge on the bottom side of the mechanism. This makes it possible to avoid interference between the released nut and the constraint bolt immediately after separation, as shown in Fig. 3(b). The operating principle of

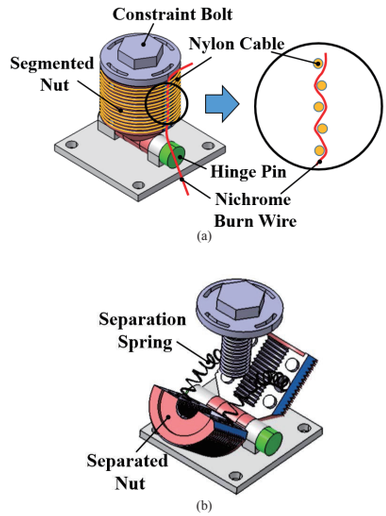

Fig. 3. Configuration of the separation nut-type holding and release mechanism proposed in this study ((a): Holding state, (b): Release state)

DOI: http://dx.doi.org/10.5139/IJASS.2015.16.4.602

the mechanism is simpler than that of the conventional one, and it does not require an outer housing with Velcro fasteners to catch the separated nut to avoid interference between the released nut and the constraint bolt after separation.

The nichrome wire was positioned on the V-shaped interface, far away from the mechanism's heat sinks to avoid heat loss and ensure a successful cut. In addition, the nichrome wire was reciprocally woven in a zigzag line through the nylon cable, as shown in Fig. 3(a). The effectiveness of the implementation method has already been verified through separation function tests under qualification temperatures [15]. This guarantees a reliable cut through the cable by avoiding inferior contact between the nichrome burn wire and the cables, which can be caused by a decrease in the cable tension due to a partial cut of the cable.

2.2 Mechanism Module for On-orbit Verification

Figure 4 shows the STEP Cube Lab configuration and location of payloads. It is based on a 1U cube satellite design, and it will fly a number of payloads for on-orbit verification of technology for future missions. The payloads [16] to be verified through the STEP mission are a variable emittance radiator, a Phase Change Material (PCM), a Micro-electro Mechanical System (MEMS) based solid propellant thruster, a Concentrating Photovoltaic (CPV) power system, and the novel non-explosive holding and release mechanism triggered by nichrome burn wire heating proposed in this study.

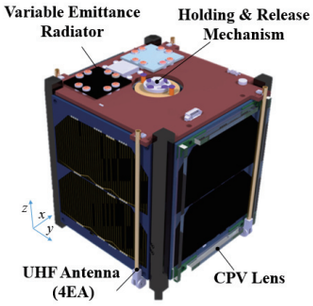

(a)

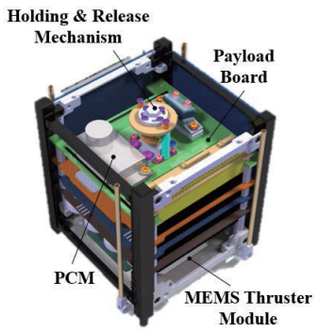

(b)

Fig. 4. Configuration of the STEP Cube Lab and location of payloads ((a): with +z panel, (b): w/o +z and side panels)

The variable emittance radiator and CPV system were located on the +z panel and side solar panels, respectively, as shown in Fig. 4(a). In the satellite configuration shown in Fig. 4 (b), +z panel and side panels are intentionally blanked for an easier understanding of the mechanism implementation. The holding and release mechanism and PCM were located on the payload panel, and the MEMS thruster module was implemented on the –z panel, although it is not clearly shown in the figure.

The current design of the satellite configuration shown in Fig. 4, is different from the preliminary design of the STEP Cube Lab configuration proposed in the previous study [15]. In the preliminary design, a single mechanism was proposed for the synchronous release of the four turnstile communication antennas, as opposed to the four activation mechanisms required for the burn wires in the conventional method. For this, the cube satellite was composed of upper and lower cube modules, and the mechanism constrained the motion of the upper cube module in the out-of-plane direction to ensure the structural safety of the satellite during lift-off. A constraint in the in-plane direction was provided by a longeron interface with an in-plane mechanical displacement limitation. When current was sent through the nichrome burn wire, the upper cube module with the antenna-holding brackets is deployed by the restoration force of the preloaded springs compressed inside the longeron beams. Subsequently, the antennas are released and are automatically deployed. However, if unexpected problems occurred in activating the newly developed mechanism on-orbit, execution of main missions to verify the normal operation of payloads cannot be expected. Therefore, to minimize the risks leading to mission failure, we decided to follow the conventional heritage for communication antenna deployments. Therefore, the final design of the STEP Cube Lab has been changed, as shown in Fig. 4, and the mechanism was not used for the communication antenna deployment, but the verification of normal operation of the mechanism on-orbit.

Figure 5 (a) and (b) show the stowed and deployed configuration of the flight model of the mechanism module to verify its normal operation under launch and on-orbit environments through STEP Cube Lab mission, respectively. The mechanism module was located on the payload panel and composed of the hinge driving separation nut-type holding and release mechanism shown in Fig.

5, a deployment status switch (Honeywell, S&C-111SM2) to judge a successful release status of the mechanism on-orbit and two compressed springs to impose a preload of 60 N in the axial direction on the mechanism. The roles of the guide beam structures on the mechanism module are to guide the movement of the compressed spring in the axial direction after a release action of the mechanism and impose a mechanical constraint in the in-plane direction of the mechanism under launch environment, which occurs at the interfaces between the holes in the circular brackets and the beam structures.

To select the separation springs compressed inside the separation nut, the torque budget, based on the ECSS rule [17], was derived by

$$T_R = 2(1.25T_{switch} + 3T_{friction} + 1.1T_{1g}) \quad (1)$$

where, T_R is the required torque to guarantee the successful release of the mechanism and the acquisition of the release signal from the deployment status switch. Torque budget values are summarized in Table 1.

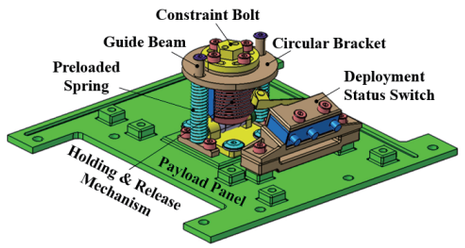

(a)

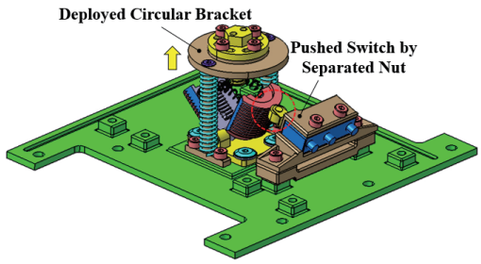

(b)

Fig. 5. Flight model of the holding and release mechanism module ((a): Holding state, (b): Release state)

Table 1. Summary of Torque Budget of the Separation Spring

Torque	Values (Nm)
T_{switch}	0.035
$T_{friction}$	4.851×10^{-5}
T_{1g}	2.742×10^{-4}
T_R	0.088

The basic functional performances of the hinge driving-type holding and release mechanism, such as successful release under qualification temperature limits and holding capability under preload condition and measured shock level, were verified and measured at the mechanism level. The structural safety and functionality of the mechanism under the launch vibration environment and on-orbit thermal vacuum environment were verified at the mechanism module level, which is the flight configuration.

3. Functional Performance Test Results at Mechanism Level

3.1 Release Function Test

Figure 6 shows the functional test configuration of the mechanism to check the stable release function of the mechanism to release the constraint bolt. To confirm the release status of the mechanism, the constraint bolt was connected to a tensioned bar to retract the bolt immediately after the activation of the mechanism. Release function tests were performed five times under the qualification temperature limits of -20 °C and 50 °C, which were obtained from (system-level) on-orbit thermal analysis of the STEP Cube Lab. Although the details of the thermal analysis were not dealt with in this study, according to the results of thermal analysis, the temperatures of the mechanism in the worst cold and worst hot cases were -4.7 °C and 31.0 °C, respectively. Based on these values, temperature margins for analysis (±5 °C) and qualifications (±10 °C)—a total of

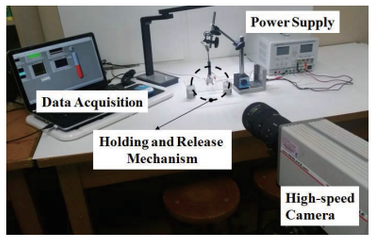

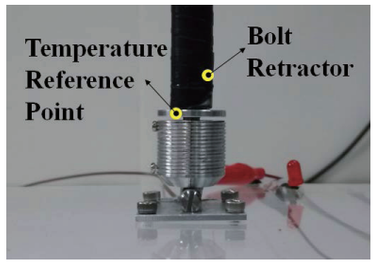

Fig. 6. Test set-up for a release function test of the demonstration model of the separation nut-type release mechanism

DOI: http://dx.doi.org/10.5139/IJASS.2015.16.4.602

±15 °C—were applied to each of the values obtained from the thermal analysis, hence the range became -20~50 °C. The target temperature was measured at the temperature reference point on the head of the constraint bolt for judging the stabilized target temperature. The low and high target temperatures were achieved using dry ice and an indirect heater, respectively.

Figure 7 shows images captured by the high-speed camera of a successful release of the mechanism triggered by the nichrome burn wire at the lower limit of the qualification temperature range, -20°C. The images indicate that the separation was successful without any interference with the constraint bolt during the release sequence.

Figure 8 shows the results of the release time measurement test obtained at air temperature and the minimum and maximum qualification temperature limits. In this test, five release function tests were performed for each temperature condition. The function tests were performed successfully.

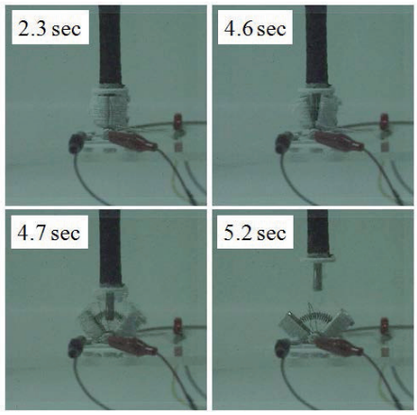

Fig. 7. Example of a successful release sequence of the mechanism

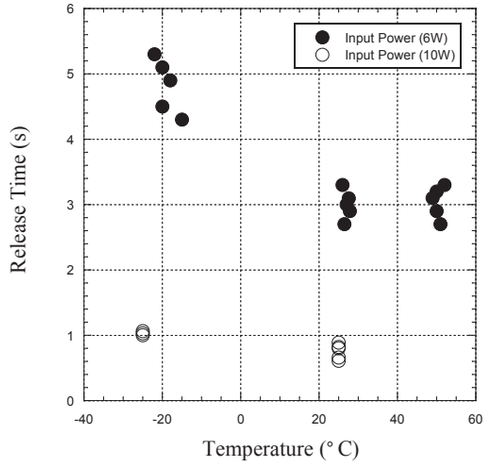

Fig. 8. Release time of the mechanism under qualification temperatures under the input power of 6W and 10W

The measured release times when the input power was 6 W, were less than approximately 3.4 s and 5.5 s under high and low qualification temperature conditions, respectively, although there was little variation. The release time measurement test results obtained at air temperature, when the input power was 10 W, were also plotted in Fig. 8. The test results indicate that the release time can be greatly reduced by increasing the input power. The burn release mechanism should be faster under vacuum than under air conditions [13]. The release function test results indicate that the current design of the mechanism can guarantee a reliable cut through the cable without failure when 6 W is provided. This can be provided by a Li-ion battery with a capability of 10 W, which can then be reduced using an electrical circuit to supply a constant current to the nichrome wire independent of the resistance of the wire and the voltage available from the spacecraft. The release function test results indicate that the mechanism functions as intended in the design under the qualification temperature limits.

3.2 Static Test

Figure 9 shows the static load test configuration for measuring the characteristics of the mechanism in constant-rate extension/compression tests using a universal testing machine (REGER Co., MTS-810) under the low and high qualification temperature limits of the mechanism. As before, the temperature reference point used to judge stabilization at the target temperature was on the bolt head. In this test, five cycles of axial extension/compression loads were applied repeatedly to the mechanism by moving the crosshead of the load tester up and down at various temperatures. The stiffness was measured to judge the structural safety of the mechanism before and after exposure to the qualification

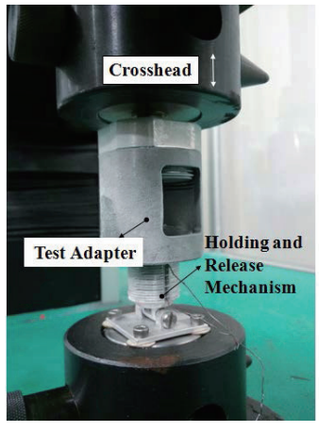

Fig. 9. Test set-up for a static load test of the demonstration model of the separation nut-type release mechanism

temperatures.

Figure 10 shows the measured stiffness values under air and qualification temperatures. The measured stiffness values after the tests, at the low and high qualification temperature limits, are also plotted in the figure for comparison with the stiffness before exposure to the qualification temperatures. The average axial stiffness of the mechanism is 4227 N/mm. On the other hand, although variations in the axial stiffness of the mechanism were observed in Fig. 10. in the low- and high-temperature cases, due to an effect of the nylon cable, which contracted and elongated with variations in the temperature, the stiffness variation, before and after exposure of the mechanism to the low and high qualification temperatures, was within 4% and thus had a negligible effect on the mechanism's performance. A release function test was also performed to check the functional performance variation of the mechanism after the static load test, and the mechanism was released successfully, without any failure, as shown in Fig. 6.

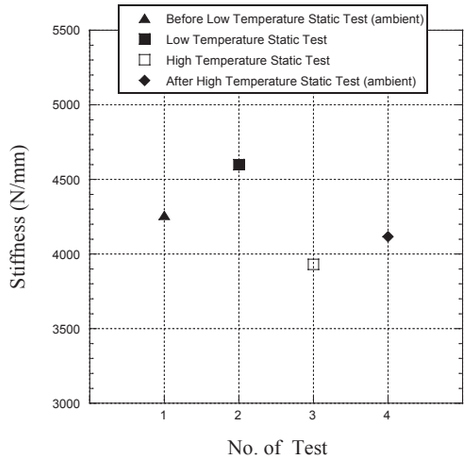

Fig. 10. Measured axial stiffness values before and after static load cycling tests at qualification temperature limits

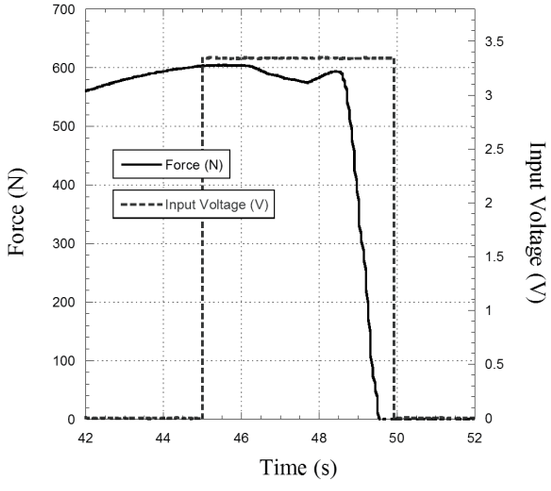

Fig. 11. Time history of loading on the mechanism and response to the triggering of the nichrome burn wire during extension of the mechanism at a constant extension rate

Figure 11 shows a time history of the load on the mechanism responding to the triggering of heating during extension of the mechanism at a constant extension rate. The test result indicates that the mechanism can guarantee a successful release under a preloaded condition on the mechanism and the mechanism is released about 3 s after burn release activation of with an input power of 6 W, which is almost the same amount of time measured from the static tests under air conditions.

Figure 12 shows the fracture test results to measure the allowable axial load on the mechanism. The mechanism is capable of holding an axial load of approximately 3200 N. This is much larger than the required allowable axial preload of 60 N for the current application. However, this also indicates that the mechanism can be applied to various deployment systems of small satellites where a high allowable axial load capability is required.

3.3 Shock Level Measurement Test

Figure 13 indicates the SRS (Shock Response Spectrum, 1/6 Octave Band) obtained from the acceleration release shock measurement test using an accelerometer (PCM piezotronics Inc., 352C03). The maximum SRS is approximately 65g when a Q factor of 10 is applied. The separated nut hitting the base, owing to the restoration force of the separation springs after the triggering of the burn wire, is responsible for most of the shock. However, the shock level

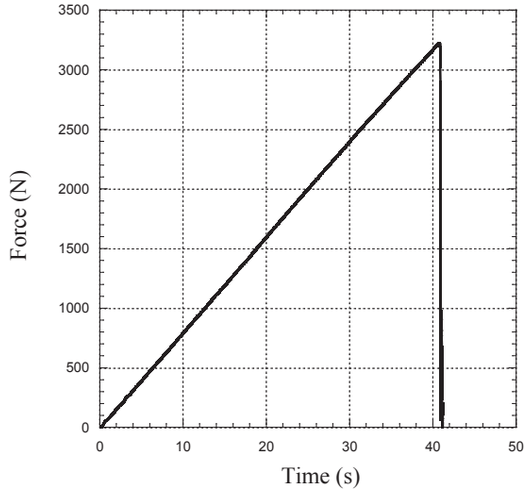

Fig. 12. Fracture test results of the mechanism

DOI: http://dx.doi.org/10.5139/IJASS.2015.16.4.602

is negligibly lower than the conventional frangibolt-type SMA actuator (FC2 Model4)), which has a maximum SRS value of 2000 g, even though the allowable axial load of the mechanism described in this paper is almost same as that of the conventional SMA actuator. The shock level can also be reduced by using separation springs with lower stiffness.

Table 2 summarizes the specification of the non-explosive separation nut-type release mechanism and the results obtained from the experimental investigations performed in this study. The results shown in the table indicate that the mechanism achieves the main development objectives of low cost, high load capacity, and negligible shock.

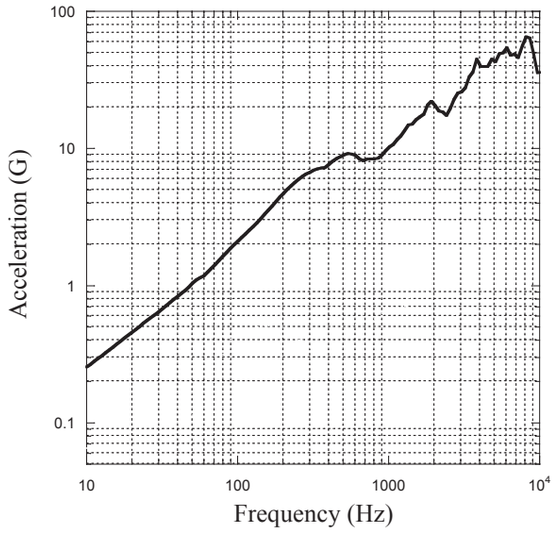

Fig. 13. Shock level measurement test results of the mechanism

4. Qualification Test Results at the Mechanism Module Level

4.1 Launch Environment Test

Figure 14 shows the vibration test configuration of the mechanism module using a vibration shaker (LING Electronics., 1216VH). In the test, sine burst, sine vibration, and random vibration loads under qualification level are applied to the mechanism module. The test level is based on the QB50 test specifications18) summarized in Table 3. The objectives of the test were to verify structural safety of the mechanism module under qualification vibration

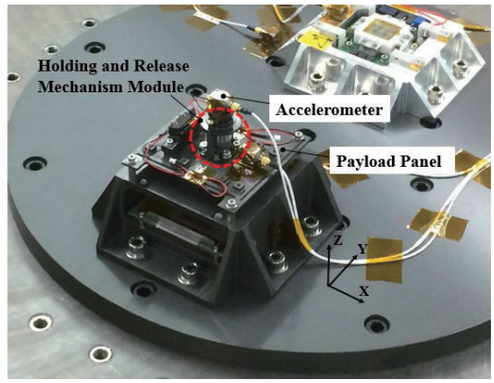

Fig. 14. Test set-up for a vibration test of the mechanism module

Table 2. Specification of the demonstration model of the holding and release mechanism

Items	Specifications	
Volume	ϕ20 mm x 27 mm	
Mass	22 g	
Allowable axial force	3200 N	
Release time (Air)	<3.5 s (25°C), <5.5 s (at -20°C)	
SRS Max.	65 g	
Required min. power	6 W	
Qualification temperature	-20°C / 50°C	
Constraint bolt	M6 (Al-6061)	
Nylon cable	Material	Nylon
	Diameter	0.3 mm
	Allowable tensile force	93 N
	Number of turns	7
Nichrome burn wire	Material	Nickel Chromium
	Diameter	0.2 mm
Release principle	Nichrome burn wire triggering	
Material	Al-6061	

loads when a preload of 60 N is applied to the mechanism, and to achieve successful release signal acquisition from the deployment status switch after vibration tests. An accelerometer, used to apply the input test loads on the mechanism, was located on the test fixture of the vibration shaker. The structural safety of the mechanism was judged by the accelerometer, installed on the bolt head, through the comparison of the low-level sine sweep test results before and after the full level vibration test. In the sine burst test, a design load of 12 g is applied to the mechanism module in each axis by the test method employing ramp up and down for 7 cycles. In addition, random and sine vibration tests were performed according to the qualification test specification in Table 3.

Table 4 compares the 1st eigen frequencies obtained from the low-level sine sweep test performed before and after vibration tests. The maximum variation of the 1st eigen frequency of the mechanism was within 2.2% for z-axis excitation. After finishing the vibration tests, release function test was also performed, and the mechanism was successfully released as show in Fig. 15. The test result indicates that the mechanism module can withstand the qualification level of launch vibration loads.

4.2 On-orbit Environment Test

Figure 16 shows the thermal vacuum test configuration of the mechanism module to confirm the stable release function of the mechanism and measure the release time under a space simulated thermal vacuum environment. The thermal vacuum test was performed using a thermal vacuum chamber (Thermotron Co., Thermotron 8200) under low and high temperatures of -35 °C and 35 °C, in contrast with those for the case of mechanism, -20~50 °C. This was because of the thermal vacuum test conditions: all of the mission payloads in the STEP Cube Lab simultaneously experienced vacuum inside a single chamber. Therefore, the temperature of the MEMS thruster was adopted as the reference

Table 3. Qualification level vibration test specifications based on the QB50

Sine Burst Test			
Amplitude (g)		Sweep	
12		Ramp up/down : 7cycles	
Sine Vibration Test			
Freq. (Hz)	Amplitude (g)		Sweep
5	1.3		2oct/min
8	2.5		
100	2.5		
Random Vibration Test			
Freq. (Hz)	Amplitude (g^2/Hz)	g_{rms}	Duration
20	0.009	8.03 g	120 sec
130	0.046		
800	0.046		
2000	0.015		

Table 4. Frequency differences of the mechanism module before and after vibration tests

Axis	**Status**	**1st Freq. (Hz)**	**Difference (%)**
x	Before	341	0.3
	After	342	
y	Before	703	0.28
	After	696	
z	Before	558	2.2
	After	546	

DOI: http://dx.doi.org/10.5139/IJASS.2015.16.4.602

temperature for the thermal vacuum test. In fact, the results of thermal analysis of the MEMS thruster in the worst cold and hot cases were -16.8 °C and 20.9 °C, respectively. In these conditions, the temperature limits (including qualification margins) were -35 °C and 35 °C, respectively, which were 15 °C lower than those of the mechanism level. However, these values of -35 °C and 35 °C were applied to the thermal vacuum test, even though the low temperature of -35 °C was relatively lower than that of the mechanism level, because the allowable temperature of the deployment status switch, -54~85 °C, has a sufficient margin. In addition, the nichrome burn wire could approach a value of 85 °C, which is the minimum temperature for releasing the mechanism, in the low-temperature case of -35 °C [13]. The target temperature was measured at the temperature reference point on the head of the constraint bolt to judge the stabilized temperature. In the test, three repeated cycles of thermal loads were applied to the mechanism module, and the release function test was performed at the coldest condition, -35°C, and at the last cycle because this was the worst condition for nichrome burn wire activation. The status of the deployment status switch was checked before the release function test at the last cycle.

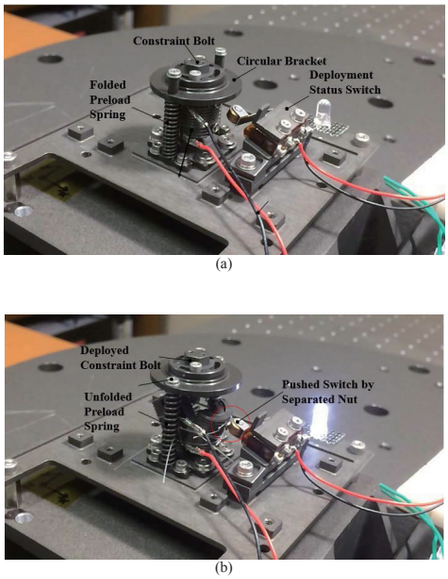

Fig. 15. Successfully released mechanism after the vibration test ((a) : Before release, (b) : After release)

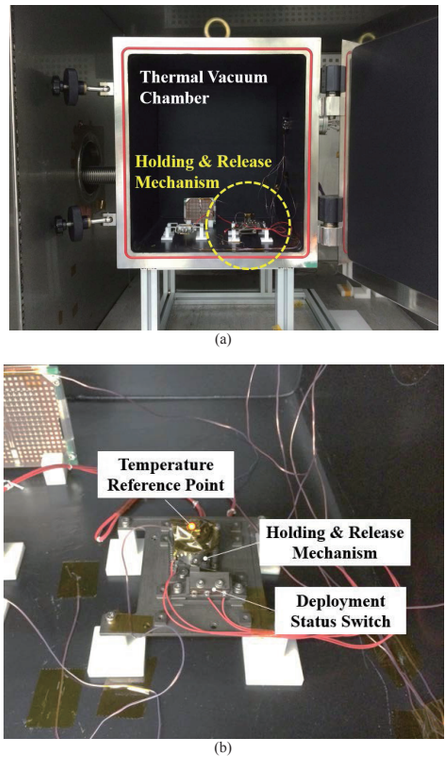

Fig. 16. Test set-up for a thermal vacuum test of the mechanism module ((a) : Thermal vacuum test set-up, (b) : Temperature sensor location)

Figure 17 indicates an example of the time profiles obtained from the deployment status switch and input voltage to the nichrome burn wire under the release function test at the coldest condition, -35°C, and at the last cycle. In the test, an input power of 10 W was applied to the mechanism, which can be provided by the selected Li-ion battery with a max power capability of 10 W. The test results indicated that the mechanism can guarantee a reliable cut through the constraint wire, without failure, under the worst conditions, and the measured release time was approximately 0.71s.

Figure 18 compares the release times obtained from the air and vacuum conditions under various temperature ranges when the applied input power is 10W. The test results under air condition were obtained before the qualification tests of the mechanism. The response time of the mechanism under

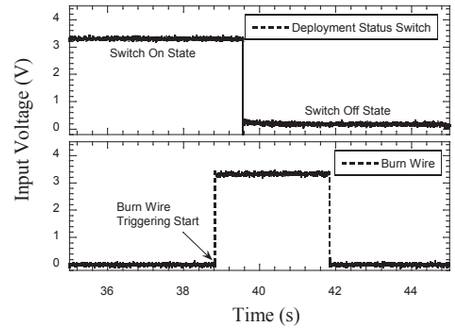

Fig. 17. Time profiles of the deployment status switch and input voltage obtained from the release function test during the thermal vacuum test

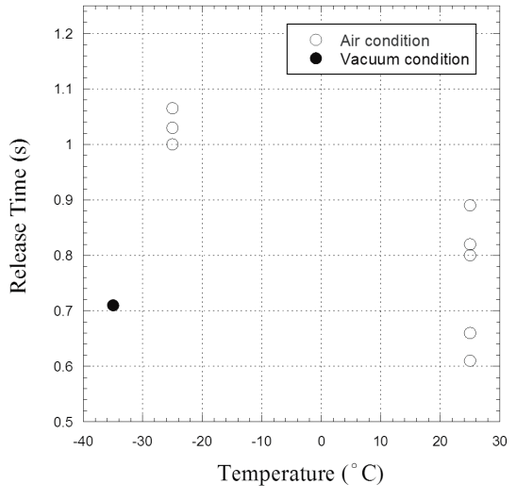

Fig. 18. Release time comparison under air and vacuum conditions when the input power was 10W

the low temperature vacuum condition show a 7 times faster response than that of the air condition although the test temperature was 15°C lower than that of the air condition.

The minimum and maximum prediction temperatures of the mechanism through on-orbit thermal analysis at system level were -19.5°C to 9°C under the worst coldest and hottest orbital conditions, respectively. The parameters used in the on-orbit thermal analysis were obtained from the thermal model correlation with the thermal balance test results although the details are not described in this paper. This means that the test temperatures applied in this study can cover the predicted operating temperature of the mechanism with a margin of 10°C.

5. Conclusion

A separation nut-type release mechanism developed for use in cube satellites has been proposed and investigated as a type of non-explosive mechanism. It has the advantage of negligible induced shocks and higher load capability than conventional nylon cable cutting mechanisms generally used for cube satellite applications. This mechanism's high axial load capability is achieved by clamping the constraint bolt to the separation nut, which is constrained by nylon cable winding. A nichrome burn wire is used to release the separation nut. The high load capability, reliable release function, and negligible shock of the mechanism were demonstrated by the static test and shock measurement test. The operating principle of the mechanism is much simpler than that of the conventional segmented nut-type mechanism proposed in a previous study, which requires the catching of the separated nuts using Velcro strips. In this study, the mechanism module design was proposed to perform the on-orbit verification of the mechanism through cube satellite missions. The reliable function and structure safety of the mechanism module, under launch and on-orbit environments, were verified through a sine burst test, sine vibration test, random vibration test and thermal vacuum test under the qualification test level. From the tests results, we concluded that the mechanism can withstand the launch loads and guarantee reliable release under severe launch and on-orbit environments. In addition, the mechanism combined with a ball-and-socket interface, as proposed in this study, opens up the possibility of applying it to other holding and release applications.

Acknowledgement

This research was supported by research fund (2015) from Chosun University.

References

[1] Woellert, K., Ehrenfreund, P., Ricco, A. J. and Hertzfeld, H. "Cubesats: Cost-effective Science and Technology Platforms for Emerging and Developing Nations", *Adv. Space Res.*, Vol. 47, No. 4, 2011, pp. 663-684.

[2] Biddy, C. and Svitek, T., "LightSail-1 Solar Sail Design and Qualification", *The 41st Aerospace Mechanisms Symposium*, Jet Propulsion Laboratory, 2012, pp. 451-463.

[3] Plaza, J. M. E., Vilan, J. A. V., Agelet, F. A., Mancheno, J. B., Estevez, M. L., Fernandez, C. M. and Ares, F. S., "Xatcobeo: Small Mechanisms for CubeSat Satellites – Antenna and Solar Array Deployment", *The 40th Aerospace Mechanisms Symposium*, 2010, pp. 415-430.

[4] Arnold, S., Armstrong, J., Person, C. and Tietz, M., "Qbx – The CubeSat Experiment", *The 26th Annual AIAA/USU Conference on Small Satellites*, 2012, SSC12-XI-4.

[5] Springmann, J., Kempke, B., Cutler, J. and Bahcivan, H., "Initial Flight Results of the RAX-2 Satellite", *The 26th Annual AIAA/USU Conference on Small Satellites*, 2012, SSC12-XI-5.

[6] Woo, S. H. and Han, J. H., "Mid frequency shock response determination by using energy flow method and time domain correction", *Shock and Vibration*, Vol. 20, No. 5, 2013, pp. 847-862.

[7] Vázquez, J. and Bueno, J. I., "Non Explosive Low Shock Reusable 20kN Hold-Down Release Actuator", *European Space Agency*, ESA - SP, Vol. 480, 2001, pp. 131-136.

[8] http://www.tiniaerospace.com

[9] Lazansky, C. and Christiansen, S., "Problems and Product Improvements in a Qualified, Flight Heritage Product", *The 38th Aerospace Mechanisms Symposium*, 2006, pp. 75-88.

[10] Oh, H. U., Jo, M. S., Lee, K. M. and Kim, D. J., "Spaceborne Tilt Mirror Mechanism and Application of Shape Memory Alloy Actuator to Implement Fail-safe Function in Emergency Mode", *Transaction of the Japan Society for Aeronautical and Space Sciences*, Vol. 55, No. 6 2012, pp. 373-378.

[11] Yano, H., Kubota, T., Miyamoto, H., Okada, T., Scheeres, D., Takagi, Y., Yoshida, K., Abe, M., Abe, S., Barnouin-Jha, O., Fujiwara, A., Hasegawa, S., Hashimoto, T., Ishiguro, M., Kato, M., Kawaguchi, J., Mukai, T., Saito, J., Sasaki, S. and Yoshikawa1, M., "Touchdown of the Hayabusa Spacecraft at the Muses-C on Itokawa", *SCIENCE*, Vol. 312, 2006, pp. 1350-1353.

[12] Nakaya, K., Konoue, K., Sawada, H., Ui, K., Okada, H., Miyashita, N., Iai, M., Urabe, T., Yamaguchi, N., Kashiwa, M., Omagari, K., Morita, I. and Matunaga, S., "Tokyo Tech Cubesat: CUTE-I-design & development of flight model and future plan", *AIAA 21st International Communications Satellite Systems Conference and Exhibit*, 2003, AIAA 2003-2388.

[13] Thurn, A., Huynh, S., Koss, S., Oppenheimer, P., Butcher, S., Schlater, J. and Hagan, P., "A Nichrome Burn Wire Release Mechanism for CubeSats", *The 41st Aerospace Mechanisms Symposium*, Jet Propulsion Laboratory, 2012, pp. 479-488.

[14] http://www.gomspace.com

[15] Oh, H. U. and Lee, M. J., "Development of a Non-explosive Segmented Nut-type Holding and Release Mechanism for Cube Satellite Applications", *Transaction of the Japan Society for Aeronautical and Space Sciences*, Vol. 58, No. 4, 2015, pp. 1-6.

[16] Oh, H. U., Jeon, S. H. and Kwon, S. C., "Structural Design and Analysis of 1U Standardized STEP Cube Lab for On-orbit Verification of Fundamental Space Technologies", *International Journal of Materials, Mechanics and Manufacturing*, Vol. 2, No. 3, 2014, pp. 239-244.

[17] European Cooperation for Space Standardization, "Space Engineering Mechanisms", *ESA Requirements and Standards Division*, 2009, ECSS-E-ST-33-01C.

[18] Singarayar, F., Reinhard, R., Asma, C., Thoemel, J., Scholz, T., Bernal, C., Weggelaar, W., Shirville, G., Kataria, D. and Richard, M., "QB50 System Requirements and Recommendations", *www.qb50.eu*, Issue 4, 2013.